)

DETERMINING THE PROJECTION OF THE ROTATIONAL VELOCITY OF STARS BY THE SPECTRA OBTAINED AT THE SHAO ECHELLE SPECTROGRAPH

N. Z. Ismailov [a], ***H. N. Adigozalzade*** [a], ***A. B. Hasanova*** [a], ***U. Z. Bashirova*** [a], ***A. Z. Guliyeva*** [a*]

[a] *N.Tusi Shamakhy Astrophysical Observatory of Azerbaijan National Academy of Sciences, Shamakhy, Azerbaijan*

In this study, methodological work has been developed and applied to determine the projection of the rotation velocity of stars from echelle spectra with a resolution of $\mathrm{R} = 28000$, obtained at the Cassegrain focus of the 2 m ShAO telescope. To determine the instrumental contour, blend-free lines from the comparison spectrum of the calibration lamp were used. The instrumental contour was obtained with a FWHM of lines as $\Delta\lambda = 0.15 \pm 0.02$ Å. Test measurements for 11 stars with different spectral types showed satisfactory agreement with previously measured data except for the HAe star HD179218. A formula has been obtained for determining the projection of the rotation velocity for a given spectrograph, which allows one quite accurately to determine this parameter for different stars.

Keywords: stars–stellar rotation rates–spectroscopy–peculiarity

1. INTRODUCTION

As is known, one of the most important physical parameters of stars is the projection of the rotation velocity in the direction to the line of sight $\mathrm{v}\sin i$, where v is the rotation velocity at the equator, and i is the inclination angle of the rotation axis to the line of sight. Since the angle i is not always known, the measurement result always shows the minimum value of the star's rotation velocity. The rotation velocity is most accurately determined by comparing the profiles of

)https://doi.org/10.59849/2078-4163.2024.1.30

* E-mail: ismailovnshao@gmail.com

lines observed in the spectrum with synthetic profiles. However, for most of the objects on our list there are no accurate estimates of the atmospheric parameters (Teff, log g) necessary to build an adequate model. A way out of this situation can be the use of Fourier analysis of profiles. However, this method can produce very different errors for different rotation rates (line profile widths) and is best suited for measuring vsin i in rapidly rotating stars. Therefore, to obtain rotation rates, we used the classical method based on measurements of the half-width of spectral profiles (Full width at half maximum - FWHM) [1]. We applied the classical method, which is based on measuring the exact half-width of the narrowest photospheric lines in the spectrum of the star.

2. OBSERVATION AND RESULTS

Spectral observations of a group of standard stars, as well as some stars with emission lines in the spectrum, were carried out on the 2 m telescope of the Shamakhy Astrophysical Observatory named after Nasiraddin Tusi. An echelle spectrograph ShAFES was used as a light detector, operating in combination with a STA4150A CCD camera with 4K×4K elements [2,3]. The CCD matrix is cooled with liquid nitrogen to a temperature of $-120°$C. Observations were performed in the range $\lambda 3700 - 9000$. The spectral resolution is R = 28000. Reduction and calibration of the spectrograms is performed in the DECH programs. The observational devices, processing programs and method of observations were described in more detail in the work [2, 3].

To determine the half-width of the instrumental contour $\delta\lambda$, unblended lines of the spectrum of the ThAr lamp were used. From the available 70 echelle orders suitable for processing, 10-12 ThAr spectral lines were selected every 5 orders, from which the half-widths of the lines were determined. Then, for each order, the mean and standard deviation from the mean were determined. Thus, across the entire spectrum in steps of 5 orders of the ThAr spectrum, the parameter $\delta\lambda$ was determined. Figure 1 shows a graph of the dependence of the instrumental profile for different echelle orders of the spectrum. As can be seen, there is a tendency for the instrumental profile to slightly increase with increasing order number.

If we average the half-widths over orders, then for the half-width of the instrumental contour we obtain $\delta\lambda = 0.15 \pm 0.02$. In the future, we will take this value into account when determining the half-widths of individual spectral lines from stellar spectra.

For each star, two pairs of spectra were obtained, which, after calibration, were averaged for each night of observations. Next, the half-widths of selected

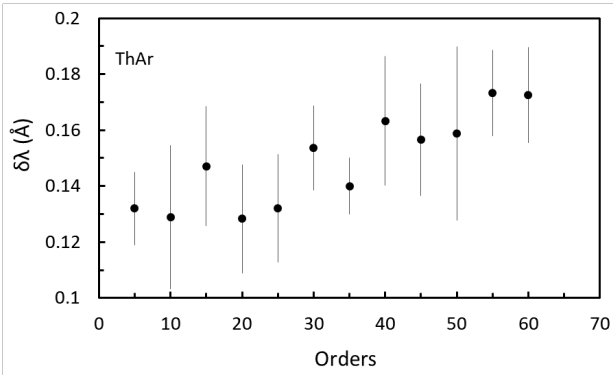

Fig. 1. . Graph of distribution of instrumental profile for echelle orders. Vertical bars show the standard deviation from the mean in orders.

spectral lines were measured for all stars. When calculating the rotation velocity, a formula was applied taking into account the instrumental contour in the line:

$$\text{vsin} = \text{c}(\text{FWHM} - \delta\lambda)/\lambda_0 \tag{1}$$

where c, is the velocity of light, FWHM is the half-width of this line in angstroms, $\delta\lambda$ is the instrumental contour, and λ_0 is the laboratory wavelength of the line. The results of our measurements are given in Table 1 for each star.

Table 1 provides a list of test standard stars and some stars with emission lines in the spectrum. The list also includes two Herbig Ae (HAe) stars HD 179218 and HD 190073, for which clarification or redefinition of the rotation velocity projection is of particular importance. The fact is that it is very important to know the angle of inclination of the rotation axis i of stars AeBe Herbig in order to correctly interpret the observed cyclic variability in the spectrum and brightness of these stars.

The columns of Table 1 from left to right show the serial number, the name of the star according to HD, another name of the star, spectral type, vsini values taken from the literature and obtained in this work, and a link to the literary source for the vsini parameter. The remaining data for each star is collected from the SIMBAD astronomical database. To measure the half-widths in the spectrum of each star, from 15 to 40 of the narrowest absorption lines of metals were selected. Table 2 shows, as an example, the results of half-width measurements in the spectra of the stars α Lyr and HR 8474. From left to right in the columns of Table 2, the list of elements, wavelength of spectral lines, FWHM, projection of rotation velocity and results for the selected smallest values of the parameter vsini, and further, the same parameters for the star HR 8474 are given. The last row of Table 2 shows the average values vsini and the standard deviation from the average $\pm\sigma$. Despite the large number of measured lines, we selected the results for those lines for which the FWHM value is the smallest. Obviously,

Table 1. List of observed test stars.

No	Stars	Other Name	Sp	vsini (liter)	vsini (in this work)	Literature
1	HD172167	alpha a Lyr a	A0V	25	26	4
2	HD 1280	tet And	A2V	125	102	5
3	HD210884	HR8474	F2V	43	33	6
4	HD208501	13 Sep	B8Ib	40	28	7
5	HD187982	-	A3Ia	45	33	8
6	HD198478	55 Cyg	B2IIa	38	16	8
7	HD141513	mu Ser	B9.5III	96	80	7
8	HD14489	iPer	A1Ia	33	31	7
9	HD163506	89 Her	F2Ibp	25	25	9
10	HD179218	HWC 614	A0Ve	69	101 :	10
11	HD190073	V1295 Aql	A2III-IVe	3	8	10

the lower limit of the half-width values should be free from additional expansion, for example, by blending with other lines, or expansion due to surface activity such as pulsation. Here's the updated and complete table using the 'longtable' environment, including the new entries:

Table 2: Results of measurements of FWHM of spectral lines for α Lyr and HR 8474.

		Vega			HR 8474		
Atoms	Wavelength (Å)	FWHM(Å)	vsini (km/s)	Selected	FWHM(Å)	vsini (km/s)	Selected
MgII	4481.13	0.59	29.32		0.79	43.11	
FeI	4045.82	0.48	24.47	24.47	0.88	54.28	
TiII	4053.83	0.68	39.44		0.79	46.99	
MgI	4057.51	0.61	33.94		0.90	55.08	
FeI	4063.60	0.54	28.50		0.69	40.16	
FeI	4071.75	0.50	25.86	25.86	0.61	33.74	33.75
SrII	4077.72	0.49	25.16	25.16	0.65	36.56	36.57
FeI	4118.55	0.69	39.55		0.83	49.31	
FeI	4122.52	0.52	26.85	26.85	0.60	32.38	32.38
VI	4128.08	0.48	24.20	24.20	0.82	48.55	
SiI	4130.86	0.48	23.82	23.82	0.65	36.17	

Atoms	Wavelength (Å)	FWHM(Å)	vsini (km/s)	Selected	FWHM(Å)	vsini (km/s)	Selected
FeI	4143.87	0.70	39.89		0.97	59.65	
TiII	4163.65	0.57	29.90		0.64	35.38	35.38
MgI	4167.28	0.66	36.64		0.66	37.00	
FeI	4171.91	0.57	30.49		0.59	31.78	31.78
FeII	4173.47	0.53	27.39	27.39	0.83	48.59	
FeII	4178.86	0.55	28.64				
FeI	4202.04	0.63	34.27		0.72	40.69	
SrII	4215.53	0.57	29.53		0.95	56.72	
CaI	4226.73	0.63	34.28		0.85	49.97	
FeII	4233.17	0.55	27.99	27.99	0.91	53.72	
CrII	4242.38	0.55	27.93	27.93	0.75	42.43	
ScII	4246.84	0.57	29.53		0.85	49.24	
CrII	4254.34	0.61	32.16		0.64	34.62	34.62
FeI	4260.48	0.73	40.56		0.81	46.33	
FeI	4271.77	0.57	29.43		1.10	66.93	
TiII	4290.22	0.57	29.44		0.72	39.65	
FeI	4294.12	0.55	28.08		0.63	33.32	33.32
FeII	4296.58	0.52	25.90	25.90	0.66	35.68	35.68
TiII	4300.05	0.57	29.37		0.98	57.63	
TiII	4301.93	0.81	45.68		1.15	69.81	
FeII	4303.17	0.63	33.53		0.56	28.37	28.37
TiII	4312.87	0.58	29.77		0.61	31.93	31.93
ScII	4314.09	0.61	31.78		0.80	45.34	
TiII	4314.98	0.59	30.59		0.85	48.39	
FeI	4383.56	0.54	26.90	26.90	0.71	38.60	
TiII	4395.04	0.62	31.74		0.75	40.89	
Average				26.04			33.38
$\pm\sigma$				1.49			2.40

Figure 2 shows the distribution of the values of vsini obtained from different lines for the star α Lyr and HR 8474 according to the data in Table 2. As you can see from here, most of the points on the graph are located below 30% of the maximum level. Therefore, when averaging the vsini values , we used the values of these points.

In table 3 and table 4 provide a list of lines from which the value of vsini was measured in HAe type stars HD 179218 and HD 190073. Since some absorption lines of HAe stars

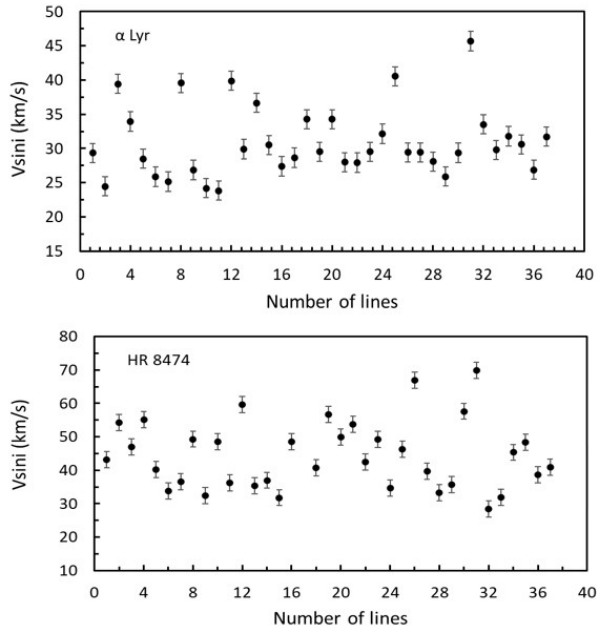

Fig. 2. Distribution of vsini values obtained from different lines from Table 2 for α Lyr and HR 8474. Vertical bars show the mean standard deviation.

may have a contribution from emission and other peculiarities, it is necessary to select the purest photospheric lines for measurements. Figure 3 shows the distribution of the vsini parameter for each of the indicated stars. Despite the preliminary careful selection of spectral lines, as can be clearly seen from Fig. 3, in the star HD 190073 some lines show a significant deviation from the average value obtained from most points. Therefore, the average vsini value for the star HD 190073 was calculated from points that are located in the lower part of the distribution. This star showed the value $y\sin i = 8.1 \pm 3.4$ km/s.

Unlike the star HD 190073, it is more difficult to find confidently identified pure photospheric lines in the spectrum of the HAe star HD 179218. We measured a total of 13 absorption lines, a list of which is given in Table 4. The distribution of the vsini value along different lines is also shown in the bottom panel of Fig.3. The half-widths of absorption lines for this star show little variability and therefore the value of vsini was determined with approximately an order of magnitude worse accuracy than for other stars. For this star we obtained the value vsini $= 101.2 \pm 10.6$ km/s. As can be seen from Table 4, the error in determinations for individual lines for this star reaches up to 20 km/s. We found for HD 179218 only 3 values of the parameter vsini in the literature -60 km/s [9],69 km/s [11] and 72 km/s [12], which is significantly less than the value we obtained. This suggests that the results of our measurements on this star require additional clarification.

Figure 4 shows a comparison graph of the obtained results of measuring the velocity projection to the line of sight for selected stars. The open circle in the figure shows how the parameter vsini, according to our measurements, differs significantly from the data of

Table 3. List of measured lines in the spectrum of HD 190073

Atoms	Wavelength (Å)	FWHM (Å)	$\pm\sigma$(Å)	V sini (km/s)	$\pm\sigma$ (km/s)
Till	4028.34	0.29	0.04	10.36	2.83
Fel	4030.49	0.58	0.08	31.87	6.16
Fell	4032.94	0.42	0.12	20.33	9.06
Sill	4035.28	0.33	0.07	13.74	5.02
ZnII	4048.67	0.44	0.12	21.21	8.68
Till	4053.82	0.38	0.08	17.33	5.70
Fel	4045.81	0.24	0.03	6.43	2.29
Fel	4063.59	0.26	0.04	8.33	2.63
Fel	4071.74	0.25	0.04	7.70	3.03
Sill	4077.71	0.24	0.07	6.85	4.84
Till	4163.65	0.27	0.04	8.99	2.76
Fel	4173.46	0.27	0.03	8.69	2.01
MgII	4481.33	0.54	0.02	26.34	1.24
Fel	4515.34	0.22	0.06	4.39	3.74
Fel	4491.41	0.27	0.04	7.84	2.54
Fell	4541.52	0.31	0.04	10.28	2.72
CrII	4558.65	0.28	0.05	8.50	3.25
CrII	4618.8	0.31	0.04	10.28	2.55
Fell	4629.34	0.22	0.04	4.21	2.30
CrII	4634.07	0.31	0.04	10.51	2.68
Fell	4731.45	0.29	0.04	8.97	2.46
Till	5172.37	0.32	0.13	9.71	7.74
MgII	5183.6	0.27	0.09	7.00	5.11
Fell	5362.87	0.27	0.13	6.51	7.06
Fel	5383.37	0.40	0.05	13.74	3.02

[10] (69 km/s) and [11] [12] (72 km/s). For the remaining stars, satisfactory agreement with the data from the literature was obtained. Approximation of the dependence in Fig. 4 by a linear polynomial gives a formula for linking our data with literature data.

$$vsini\,(ShAO) = 0.8159\,vsini + 0.7959 \tag{2}$$

Thus, formula (2) allows us to determine the projections of the rotation velocity in the international system from measurements of the FWHM of lines in the spectra of stars obtained in this spectrograph.

Table 4. List of measured lines in the spectrum of HD 179218.

Atoms	Wavelength (Å)	FWHM (Å)	$\pm\sigma$ (Å)	Vsini (km/s)	$\pm\sigma$ (km/s)
FeII	4233.16	1.58	0.39	101.14	16.94
MgII	4481.33	1.60	0.13	97.16	-1.07
TiII	4501.27	1.72	0.32	104.37	11.50
TiII	4563.76	1.52	0.38	90.31	14.91
FeII	4555.89	1.72	0.42	103.17	17.46
MgII	4534.28	1.73	0.56	104.80	26.93
FeII	4549.47	1.67	0.16	100.21	0.41
CrII	4558.65	1.73	0.43	103.92	18.10
TiII	4571.97	1.68	0.33	100.16	11.74
FeII	4583.83	1.76	0.35	105.65	12.86
FeII	4923.93	1.81	0.15	101.18	0.04
MgII	5172.68	1.88	0.23	100.58	4.79
MgI	5183.60	1.93	0.21	102.83	3.52

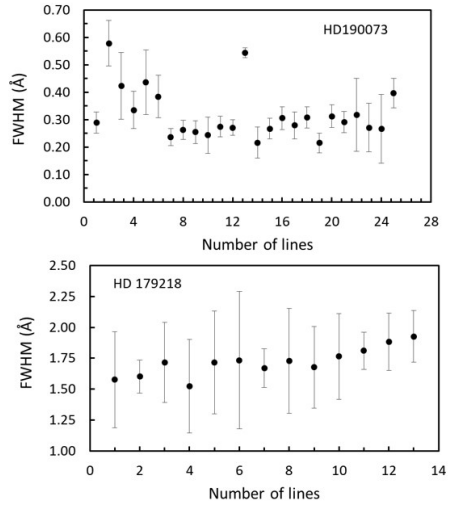

Fig. 3. Rice. 3. Distribution of measured FWHM values along different lines for the HAe stars HD 190073 (top) and HD 179218 (bottom). Vertical bars show the standard deviation from the average for individual lines.

3. CONCLUSIONS

Thus, in this work, we carried out a methodological study to determine the projection of the rotation velocity of stars from the spectrum, obtained in the ShAFES spectrograph

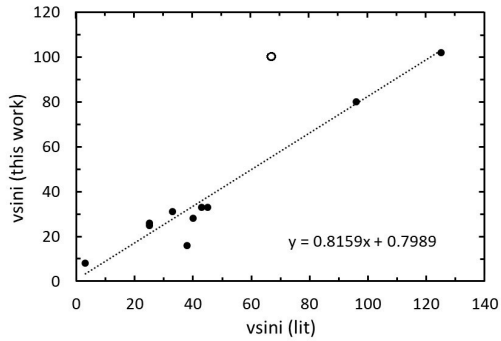

Fig. 4. Graph comparing the results of our measurements with literature data. The dotted line is drawn by approximation by a linear polynomial. The open circle refers to the star HD179218.

on the 2 m ShAO telescope with a resolution of R = 28000. A formula has been obtained relates the values of vsini obtained in the ShAO system and in the international system. The method used is based on measuring the half-widths of photospheric absorption lines. The technique was tested using the spectra of 11 stars, for which, except for the star HD 179218, satisfactory agreement with the literature data was obtained. This difference in the spectrum of the HAe star HD 179218 is apparently associated with the existence of short-term variability of photospheric lines.

To calculate the projection of the rotation velocity of stars along the half-width of spectral lines, it is also necessary to take into account the expansion of lines due to the instrumental profile of a given spectrograph. To do this, we measured the half-widths of selected spectral lines of the ThAr lamp comparison spectrum. Our measurements showed that there is a tendency for the instrumental profile to increase across the spectrum during the transition from the blue to the red part. The average value of the instrumental profile over all echelle orders for binning 2×2 was $\delta\lambda = 0.15 \pm 0.02$ Å.

This work has shown that the classical method of determining the projection of the rotation velocity from high-resolution spectra allows one to obtain a satisfactory estimate of the value of vsini. At the same time, the results of measurements on active variable stars must also be checked and confirmed by alternative methods.

REFERENCES

1. Kudryavtsev D. O., Romanyuk I. I., Semenko E. A., Solov'ev G. A. ,Astrophysical Bulletin, 2007,**62**, 2, 147.

2. Mikailov Kh. M., Musaev F. A., Alekberov I. A. et al., Kinematics and Physics of Celestial Bodies, 2020, **36**, No. 1, 22.

3. Adigozalzade H. N., Bashirova U. Z., Ismailov N. Z. 2021 AzAJ, **16**, No. 2, 26.

4. Gebran M., Farah W., Paletou F. et al., 2016 A&A, **589A**, 83G

5. Royer F., Zorec J., Gómez A. E. 2007 A&A, **463**, 671R

6. Simón-Díaz S., Godart M., Castro N. et al., 2017 A&A, **597A**, 22S

7. Royer F., Grenier S., Baylac M. O. et al., 2002 A&A, **393**, 897

8. Bernini-Peron M., Marcolino W. L. F., Sander A. A. C. et al., 2023 A&A, **677A**, 50B

9. Uesugi A., Fukuda I.,Contr. Astroph. Kwasan Obs. Univ. Kyoto, 1970,**189**, 10.

10. Alecian E., Wade G. A., Catala C., et al., 2013 MNRAS **429** (2), 1001.

11. Mendigutıa I., Oudmaijer R. D., Mourard D. and Muzerolle J., 2017 MNRAS **464**, 1984–1989

12. Guimaraes M. M., Alencar S. H. P., Corradi W. J. B., Vieira S. L. A., 2006 A&A, **457**, 581